Biochemical and Biophysical Research Communications 767 (2025) 151896

Contents lists available at ScienceDirect

Biochemical and Biophysical Research Communications

journal homepage: www.elsevier.com/locate/ybbrc

Development of a human RPE *In vitro* model with AMD-like features reveals blue light-induced modulation of the endocannabinoid system

Camilla Di Meo [a,b,1], Annamaria Tisi [a,1], Anna Rita Lizzi [a], Sakthimala Palaniappan [a], Fanny Pulcini [a], Benedetta Cinque [d], Simona Delle Monache [a], Marc Nazarè [e], Eric Hsu [c], Cinzia Rapino [b,2], Mauro Maccarrone [a,f,*,2]

[a] Department of Biotechnological and Applied Clinical Sciences, University of L'Aquila, 67100, L'Aquila, Italy
[b] Department of Veterinary Medicine, University of Teramo, Teramo, Italy
[c] InMed Pharmaceuticals Inc., Vancouver, BC, Canada
[d] Department of Life, Health & Environmental Sciences, University of L'Aquila, 67100, L'Aquila, Italy
[e] Leibniz Research Institute for Molecular Pharmacology (FMP), Campus Berlin-Buch, 13125, Berlin, Germany
[f] European Center for Brain Research (CERC), Santa Lucia Foundation IRCCS, Rome, Italy

A B S T R A C T

Blue light (BL) is a known risk factor for age-related macular degeneration (AMD), a retinal pathology where damage to the retinal pigment epithelium (RPE) is one of the earliest events. While the endocannabinoid system (ECS) is implicated in various physio-pathological conditions of the retina, its role in BL-injured RPE has not yet been addressed. To fill this gap, we developed an *in vitro* model of BL-induced human RPE damage showing key features of AMD: cytotoxicity, cell cycle arrest, oxidative stress, inflammation, and cellular senescence. Notably, our model demonstrates modulation of gene and protein expression of specific ECS elements, particularly cannabinoid receptors 1 and 2 (CB_1 and CB_2), thus providing unprecedented evidence of ECS dysregulation in RPE cells upon BL exposure.

1. Introduction

Light pollution, and particularly blue light (BL) emitted by light-emitting diodes (LEDs), is emerging as a major risk factor for the development and progression of age-related macular degeneration (AMD), a retinal degenerative disease affecting the retinal pigment epithelium (RPE) which is expected to become the leading cause of blindness and vision impairment by 2050 [1]. This is a growing concern in modern society due to the increasing use of LED-based technologies, such as computers, smartphones, tablets, televisions, and general LED illuminations [2]. As a result, several studies are focusing on the mechanisms underlying BL-induced phototoxicity and possible protective strategies [3].

Accumulated evidence indicates that bioactive lipids may be key molecules in regulating pathological processes of several diseases, including retinal degenerative disorders [4–12]. Among them, endocannabinoids (eCBs) act through target receptors and are regulated by metabolic enzymes that altogether form the so-called "endocannabinoid system" (ECS), which plays a pivotal role in the homeostasis of the human body [13]. Different receptors can be activated by eCBs, including cannabinoid receptors 1 (CB_1) and 2 (CB_2), G protein-coupled receptor 55 (GPR55), transient receptor potential vanilloid receptor 1 (TRPV1), and peroxisome proliferator-activated nuclear receptors (PPARs) α, δ, γ [9]. The major eCBs anandamide (*N*-arachidonoylethanolamine, AEA) and 2-arachidonoylglycerol (2-AG) are synthesized by specific lipases, mainly *N*-acyl phosphatidylethanolamines-specific phospholipase D (NAPE-PLD) and diacylglycerol lipases α and β (DAGLα, DAGLβ), respectively [9]. AEA and 2-AG are then mainly hydrolyzed by fatty acid amide hydrolase (FAAH) and monoacylglycerol lipase (MAGL), respectively [9]. Notably, almost all retinal cell types across different species express some elements of the ECS, which is a key molecular network involved in retinal homeostasis, as well as neurotransmission and regulation of retinal ion channel activity [14]. However, the ECS has never been investigated in the RPE directly subjected to light damage. Therefore, in the present study we sought to fill this relevant gap by developing a suitable *in vitro* model of BL-induced RPE damage with AMD-like features, and to investigate potential alterations in the ECS due to BL phototoxicity.

* Corresponding author. Department of Biotechnological and Applied Clinical Sciences, University of L'Aquila, 67100, L'Aquila, Italy
E-mail address: mauro.maccarrone@univaq.it (M. Maccarrone).
[1] Co-first authors.
[2] Co-senior authors.

https://doi.org/10.1016/j.bbrc.2025.151896
Received 16 April 2025; Received in revised form 24 April 2025; Accepted 24 April 2025
Available online 25 April 2025

2. Materials and methods

2.1. Cell culture and blue light (BL) setting

Human RPE cells (ARPE-19) were purchased from ATCC (CRL-2302, American Type Culture Collection, ATCC, Manassas, VA, USA) and cultured at 37 °C in a humidified 5 % CO_2 atmosphere in DMEM/F12, supplemented with 10 % heat-inactivated foetal bovine serum (FBS), 100 U/mL penicillin, 100 μg/mL streptomycin and 2 mM glutamine, according to the manufacturer's instructions. ARPE-19 cells were subjected to two blue light (BL) damage paradigms.

(i) BL1 (short exposure, high light energy): 30 Watt for 80 min;
(ii) BL2 (long exposure, low light energy): 4.8 Watt for 8h.

The distance from the light stimulator to the cells was 6 cm. After irradiation, the cells were allowed to recover for 24h, 48h and 72h.

2.2. MTT cytotoxicity assay and trypan blue exclusion test

Cells were seeded into 96-well plates (5×10^3/well). Cell viability was assessed by the 3-[4,5-dimethylthiazol-2-yl]-2,5-diphenyl tetrazolium bromide (MTT; Sigma Aldrich) assay. Cells were incubated with MTT solution, which was discarded after 4h and replaced with isopropanol, to dissolve the formazan crystals. Cell viability, related to metabolic active cells, was calculated by subtracting the 630 nm OD background from the 570 nm [15].

For the Trypan Blue Exclusion Test, cells resuspension in DMEM/F12 was prepared 1:1 with Trypan Blue solution 0,4 % (Gibco, Thermo Fisher Scientific, Waltham, Massachusetts, USA) and clear cells (not stained with blue) were counted by using a manual hemocytometer.

2.3. Cell cycle distribution and apoptotic cell detection by flow cytometry analysis

Cells were seeded in 24-well plates (1.5×10^4/well). After collection, cells were washed twice with PBS and fixed with 70 % ethanol in PBS at 4 °C for 30 min. Then, 10^6 cells/mL were washed twice with PBS, and resuspended with a solution containing 50 μg/mL PI, 0.1 % Nonidet-P40, and RNase A (6 μg/10^6 cell) for 30 min in the dark at 4 °C. Data from 10,000 events *per* sample were collected and analyzed using a FACS Calibur instrument (BD Biosciences) equipped with cell cycle analysis software (Modfit LT for Mac V3.0) to calculate the percentages of cells in the G1, G2/M, and S phases. The apoptotic cells were determined by their hypochromic subdiploid nuclei staining profiles and analyzed using Cell Quest software program (BD Instruments Inc.) [16].

2.4. Reactive oxygen species (ROS) assay

Cells were seeded in 96-well plates (5×10^3/well), stained with CellROX Oxidative Stress (1 μM) and transferred to the temperature- and CO_2-controlled IncuCyte ZOOM® (Incucyte S3 2018C). Images were taken with an average scan interval of 24h until 72h with excitation/emission maxima at 640/665 nm. Fluorescent objects were quantified using the IncuCyte® integrated analysis software [17].

2.5. Cell senescence assay

Cells were seeded in 24-well plates (1.5×10^4/well). Senescence was determined through the β-galactosidase staining kit (Cell Signaling Technology) [18]. The plate was rinsed with PBS and fixed with 1X fixative solution for 15 min and then incubated with the β-galactosidase staining solution at 37 °C for 16h. Senescent cells were identified as blue-stained cells under light microscopy (Zeiss Telaval 31) and counted (at x20 magnification) in at least 4 randomly chosen fields.

2.6. ELISA assay

Cells were seeded in T25 flasks (3×10^5). Conditioned media (CM) from cells were collected and then concentrated by Vivaspin 3 kDa (Euroclone Milan, Italy). The following ELISA kits were used: human IL-10 and IL-4 (Abcam, Cambridge, MA, USA), human IL-1β and TNF-α (RayBiotech Life, Peachtree Corners, GA). The levels of cytokines were normalized with respect to the number of cells.

2.7. Quantitative real-time polymerase chain reaction (RT-qPCR)

Cells were seeded in 6-well plates (2×10^5/well). Cell pellets were collected, and RNA extraction was performed by QIAzol Lysis Reagent (Qiagen, Hilden, Germany). RNA extracted was quantified with a NanoDrop™ 2000/2000c Spectrophotometer (Thermo Fisher Scientific Company, Waltham, MA, USA) and reverse-transcribed (500 ng) through the RevertAid H Minus First Strand cDNA Synthesis (Thermo Fisher Scientific), following incubation in thermocycler at 65 °C (5 min), 25 °C (5 min), 42 °C (60 min) and 70 °C (5 min). RT-qPCR was performed as previously described [19]. Primers used are summarized in Table S1. Data obtained were normalized to the endogenous reference genes β-actin and glyceraldehyde-3-phosphate dehydrogenase (GAPDH). The relative genes abundance was calculated with the ΔΔCt method.

2.8. Protein extraction and western blotting

Cells were seeded in 6-well plates (2×10^5/well). Cells were collected and resuspended in 30 μL of lysis buffer, as previously detailed [16]. Lysates were quantified with Bradford colorimetric method. 60 μg of proteins were loaded in Bolt 4–12 % Bis-Tris Plus (Thermofisher Scientific) and transferred using iBlot™ 3 Transfer Stacks, midi, PVDF (Thermo Fisher Scientific) in iBlot™ 3 dry transfer system. The membrane was washed for 5 min in TBS-T (10 mM Tris–HCl, 150 mM NaCl, 0.1 % Tween 20 pH 7.6) and aspecific bindings were blocked with 5 % non-fat dry milk in TBS-T for 1h at room temperature (RT) on a shaker platform. Primary antibodies, detailed in Table S2, were diluted in 5 % non-fat dry milk or 5 % Bovine Serum Albumine (BSA) and incubated overnight at 4 °C.

Membranes were developed using Super Signal West Pico Plus (Thermo Fisher Scientific) or Super Signal West Atto Ultimate Sensitivity (Thermo Fisher Scientific) chemiluminescent substrates and the bands were detected using a ChemiDoc XRS plus imaging system (Bio-Rad Laboratories). The densitometry was performed using Image J software and results were normalized to GAPDH.

2.9. Live cell imaging of CB_2 via 8-SiR probe

Cells were seeded in chambered coverslips (Ibidi) (5×10^3/well), treated with the fluorescent CB_2 agonist probe (8-SiR) (0.6 μM) and immediately analyzed by using a TCS SP5 confocal microscope [20]. To perform live imaging, images were recorded every 15 s for 30 min. Images were exported as TIFF files and a video was created to visualize time-related 8-SiR signal.

2.10. Statistical analysis

Data were analyzed by GraphPad Prism 8 program (GraphPad Software, La Jolla, CA, USA) and plotted as means ± standard error of the mean (SEM). Statistical analyses were performed using the Unpaired *t*-test or the Multiple *t*-test, followed by the correction of Bonferroni-Dunn. A value of $p < 0.05$ was considered statistically significant.

3. Results

3.1. Set up of the in vitro BL-induced RPE damage model

To establish the optimal *in vitro* model of BL-induced RPE damage, cell viability and metabolic activity were assessed through Trypan Blue exclusion test and MTT assay, respectively. ARPE-19 cells were exposed to two different models of BL irradiation (450–470 nm): (i) BL paradigm 1 (BL1) involved high energy (30 Watts) for a short duration (80 min), and (ii) BL paradigm 2 (BL2) used lower energy (4.8 Watts) for a longer duration (8 h). In both cases, cells were allowed to recover at 3 time-points (24 h, 48 h and 72 h) after irradiation. The results showed a significant decrease in cell viability in both models, at 48h (~40 %) and 72h (~40 %) of recovery for BL1, and only at 72h of recovery for BL2 (~30 %) - as shown in Fig. 1A and B and in Table S1. BL1 also led to a significant decrease in the number of viable cells at the same time points (Fig. 1C), whereas BL2 failed in that (Fig. 1D).

On this basis, BL1 with 48h of recovery (defined as "BL") was selected for subsequent molecular and biochemical analyses.

3.2. BL induced cell cycle arrest, oxidative stress, cellular senescence and inflammation in the in vitro RPE damage model

We next investigated the main hallmarks of AMD associated with RPE cells. BL led to ARPE-19 cell cycle arrest, evaluated through flow cytometry, with a significant decrease in G1 and a significant increase in G2/M and S phases (Fig. 2A). A similar result was observed in BL-injured cells even after 24h and 72h, except for the S phase at 24h (Fig. S1). Of note, BL did not induce apoptosis, as shown by the analysis of cell debris (Fig. 2A and Fig. S1).

Additionally, BL exposure induced a significant increase of ROS production, a key hallmark of AMD [21], in ARPE-19 cells after 48h of recovery compared to control, as shown by the increased red fluorescent signal of the CellROX probe (Fig. 2B). A significant ROS increase was also observed upon recovery of 24h and 72h post-irradiation (Fig. S2A).

Next, the onset of cellular senescence - an important feature of AMD pathology [22] - was evaluated in the BL model, by using the β-galactosidase assay. A significant increase in the number of β-galactosidase (+) ARPE-19 cells was observed 48h after BL (Fig. 2C). Cellular senescence was not detected 24h after BL, but it persisted for up to 72h (Fig. S2B).

Finally, inflammation was investigated by quantifying the levels of key pro-inflammatory (IL-1β, TNFα) and anti-inflammatory (IL-4, IL-10) cytokines, known to contribute to the progression of AMD [23–25]. A significant increase in the release of TNFα, along with a trend in the increase of IL-1β levels, was observed in ARPE-19 cells exposed to BL damage (Fig. 2D). Interestingly, the latter cells showed a significant increase in IL-4 levels and a decrease in IL-10 levels compared to controls (Fig. 2D).

Overall, BL-irradiated ARPE-19 cells exhibited key hallmarks of AMD, making them a suitable model for molecular investigations into RPE photo-toxicity in the context of AMD pathology.

3.3. BL modulated gene expression of selected ECS elements in the in vitro RPE damage model

After establishing the BL-induced RPE damage with AMD-like features, we aimed to unravel the possible effects of BL on the main eCB-binding receptors and metabolic enzymes at the gene level through RT-qPCR (Fig. 3A and B). ARPE-19 cells exposed to BL showed a

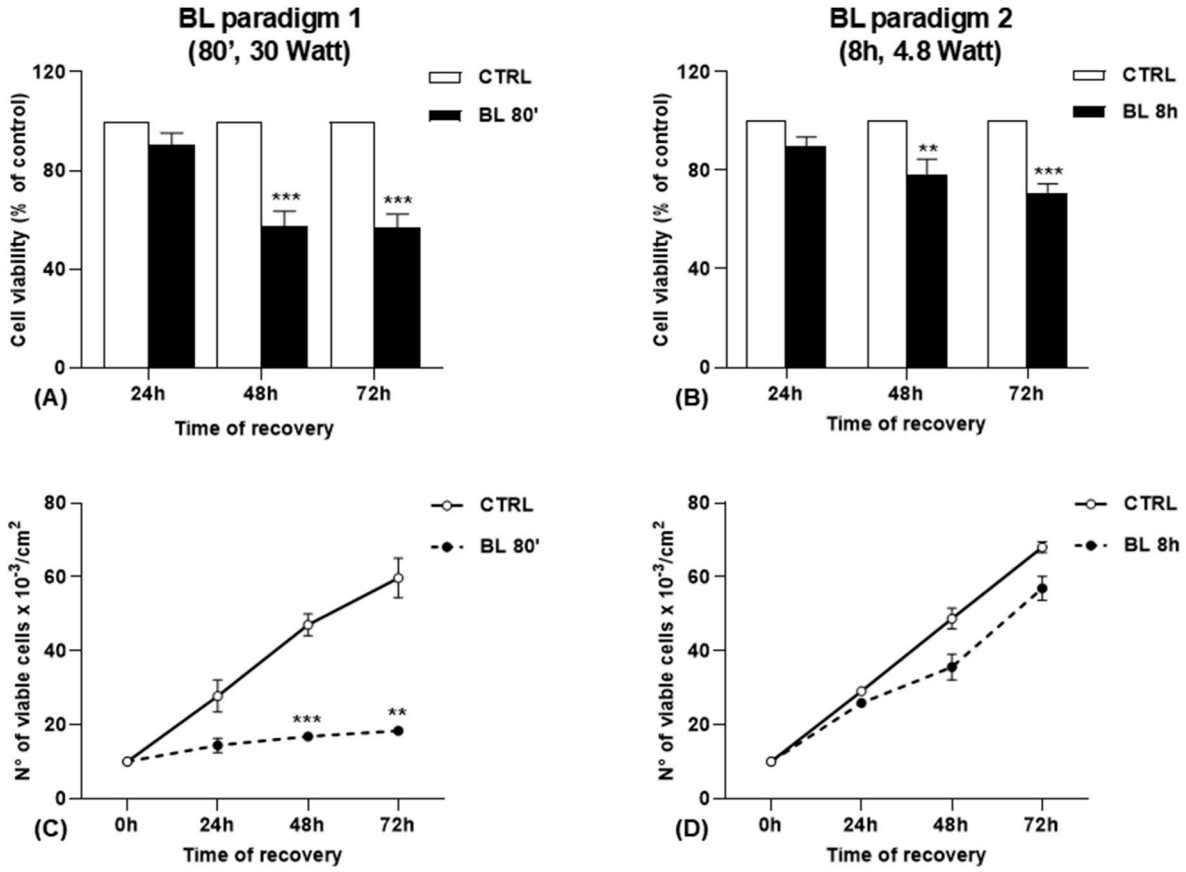

Fig. 1. Effect of BL paradigm 1 (BL1) and 2 (BL2) on ARPE-19 cell viability. MTT assay and Trypan Blue exclusion test in (A)–(C) BL1 (high energy, short exposure); and **(B)–(D) BL2 (low energy, long exposure).** Data are shown as the mean ± SEM of three independent experiments (N = 3). Statistical analysis was performed by Multiple *t*-test, followed by correction of Bonferroni-Dunn (**p < 0.01; ***p < 0.001 *vs* CTRL).

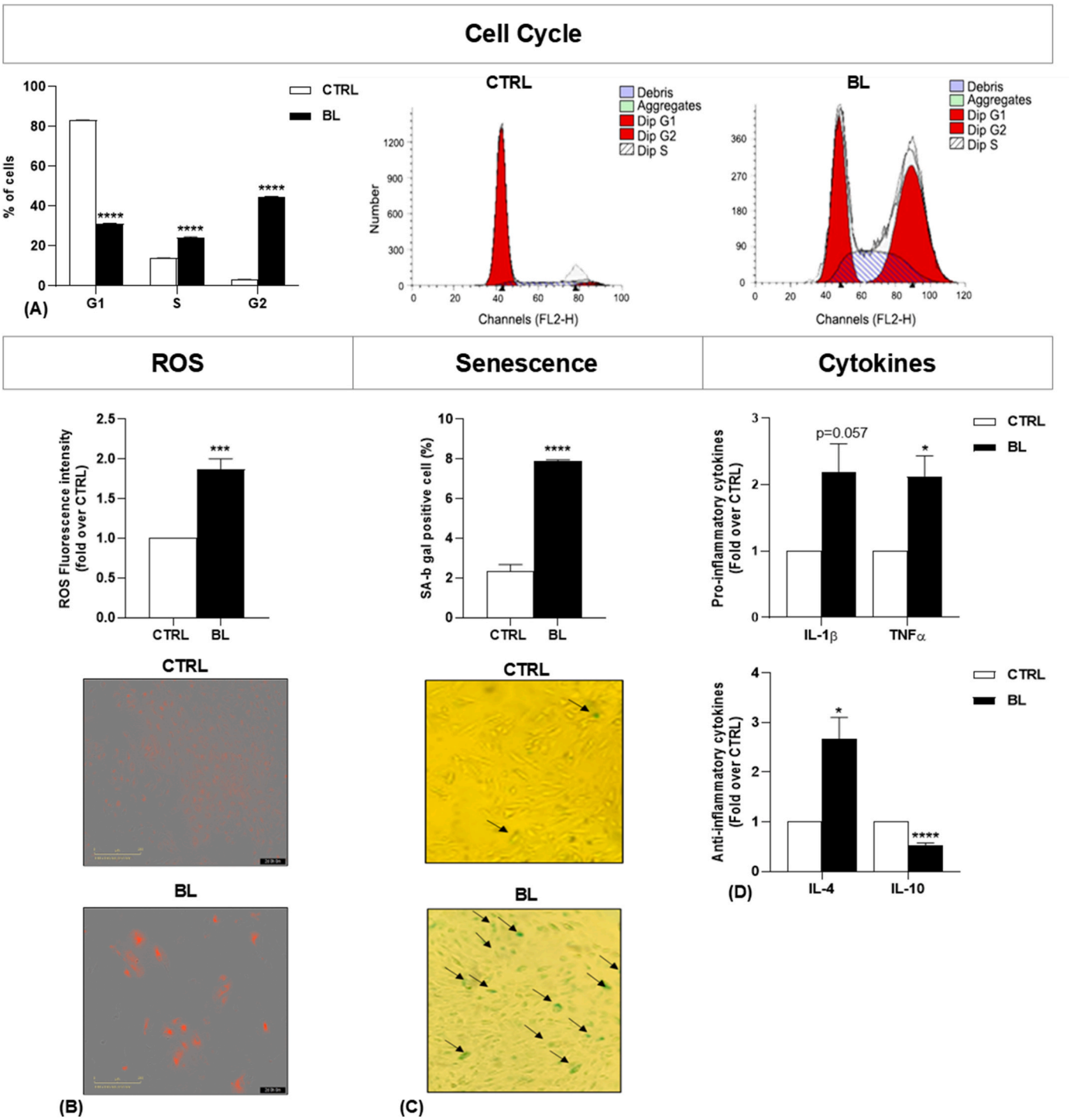

Fig. 2. Effect of BL on ARPE-19 cell cycle distribution, intracellular ROS production, pro-inflammatory cytokines release and cell senescence. (A) Percentage of cells evaluated by flow cytometry analysis in cell cycle phases; **(B)** ROS quantification through IncuCyte imaging and representative microscopic images; **(C)** Percentage of SA-β-Gal positive cells and representative microscopic images of the staining in BL-irradiated *vs* CTRL cells following 48h of recovery; **(D)** IL-1β, IL-4 and TNFα levels normalized with respect to the number of cells. Data are shown as the mean ± SEM of three or four independent experiments (N = 3–4). Statistical analysis was performed by Unpaired *t*-test and Multiple *t*-test, followed by correction of Bonferroni-Dunn (*p < 0.05; ***p < 0.001; ****p < 0.0001 *vs* CTRL).

significant increase in the expression of CB_1 and CB_2 genes, as well as of PPARγ, while a significant decrease in NAPE-PLD gene expression was observed (Fig. 3A and B). None of the other ECS elements was significantly affected, suggesting a distinct modulation of specific eCB-binding receptors and enzymes in the *in vitro* model of BL-induced RPE damage.

3.4. BL decreased CB_1 and increased CB_2 protein expression in the in vitro RPE-damage model

Based on the observed modulations in gene expression levels, we next evaluated the protein expression of CB_1, CB_2, PPARγ and NAPE-PLD through Western blotting. Interestingly, BL cells showed a significant decrease in the protein expression of CB_1 (Fig. 4A) and a significant

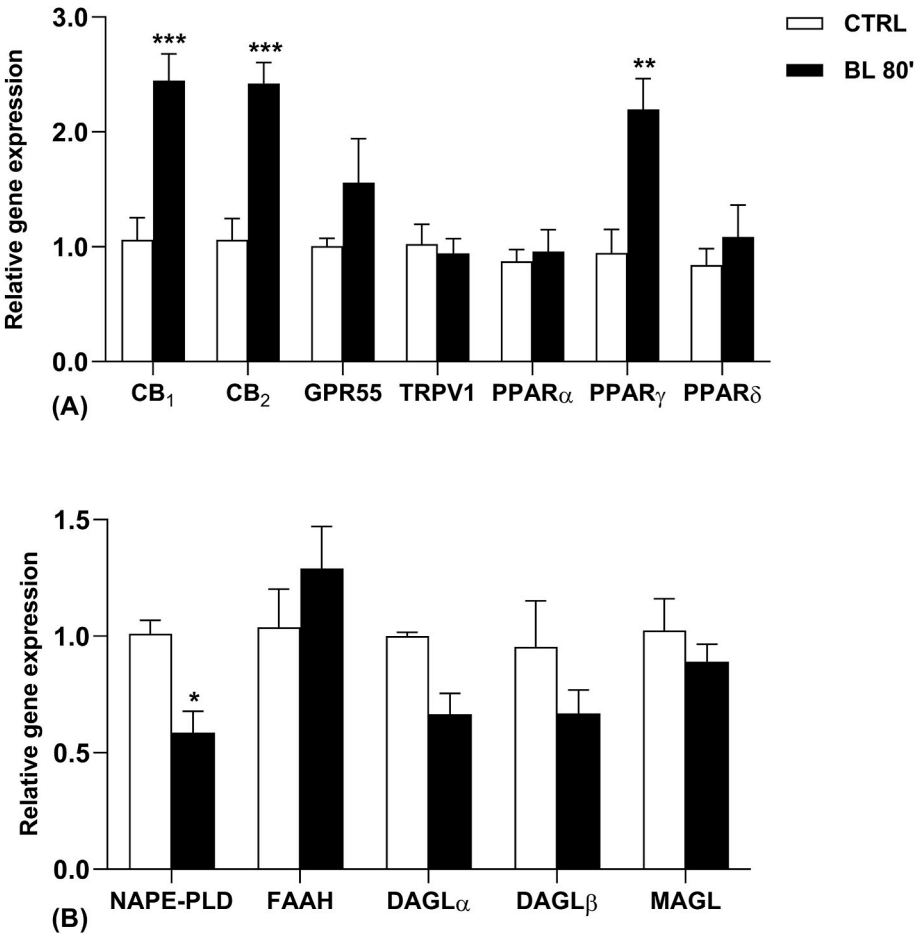

Fig. 3. BL effect on gene expression of the main ECS elements in ARPE-19 cells. RT-qPCR results for **(A)** eCBs-binding receptors (CB1, CB2, GPR55, TRPV1, PPARα/γ/δ), and **(B)** eCB metabolic enzymes (NAPE-PLD, FAAH, DAGLα/β, MAGL) in BL and CTRL cells. Data are shown as the mean ± SEM of three independent experiments (N = 3) and are expressed as 2(-ΔΔCt). Statistical analysis was performed by Multiple *t*-test, followed by correction of Bonferroni-Dunn method (*p < 0.05; **p < 0.01; ***p < 0.001 vs CTRL).

increase in that of CB_2 compared to control cells (Fig. 4B). Instead, PPARγ and NAPE-PLD expression was not significantly affected at the protein level (Fig. 4C and D). Notably, the results obtained for the protein expression of CB_2 in BL-exposed ARPE-19 cells were consistent with the gene expression data, both indicating an increase upon BL damage.

To further investigate CB_2 protein expression, we performed live cell imaging experiments using a recently developed CB_2-selective fluorescent probe, called 8-SiR (Gazzi et al., 2022). These experiments revealed higher CB_2 expression (in red) in BL-exposed cells compared to controls, as shown in Fig. 4E and in the time-lapse videos provided as supplementary files.

4. Discussion

The ECS is emerging as a key molecular signalling system under both physiological and pathological conditions of the retina [26]. This evidence is particularly relevant in the context of AMD, where blue light (BL) exposure is widely recognized as a risk factor [27]. However, ECS-related changes induced by light damage in the RPE have not yet been investigated, representing a relevant gap of knowledge.

Against this background, in the present study we investigated whether BL phototoxicity affects eCB signalling in RPE cells. To this end, we developed an *in vitro* BL model using ARPE-19 cells to represent human RPE. To enhance the translational impact of our findings, we first assessed whether our BL model could replicate the key features of AMD. The viability of ARPE-19 cells was reduced by BL exposure, which was associated with cell cycle arrest, RPE cytotoxicity and oxidative stress. Importantly, ARPE-19 cells exhibited perturbation in cytokine release and cellular senescence, all data that support the suitability of our BL system as an *in vitro* AMD-like model.

Then, we performed gene profiling of the major ECS components, including receptors and metabolic enzymes of AEA and 2-AG. Our data demonstrate for the first time that: (i) the genes of the major ECS elements are expressed in ARPE-19 cells, thus extending previous findings on some ECS elements only [14,28,29]; and (ii) BL upregulates gene expression of specific eCBs-binding receptors (CB_1, CB_2, and PPARγ), while downregulating that of NAPE-PLD, the biosynthetic enzyme of AEA. Importantly, protein analysis of the modulated genes revealed that only CB_1 and CB_2 proteins were affected by BL. In particular, CB_1 was upregulated at the gene level, yet it was downregulated at the protein level. This apparent discrepancy may be related to additional molecular processes, such as post-transcriptional mechanisms or changes in receptor turnover, as already observed by others and by us [19,30–32]. Unlike CB_1, CB_2 was upregulated at both gene and protein levels. The latter result was further confirmed by using an innovative live-cell imaging methodology based on the highly permeable and CB_2 selective fluorescent probe 8-SiR (Fig. 4E), that is devoid of limitations often associated to the use of CB_2 antibodies [33,34]. It should be noted that the upregulation of CB_1 and CB_2 was also found in a previous study by our group using an animal model of light damage [35]; however, this analysis was performed on whole retinal lysates, making it difficult to assess the specific effects of light damage on the RPE.

Taken together, our findings provide the first systematic analysis of

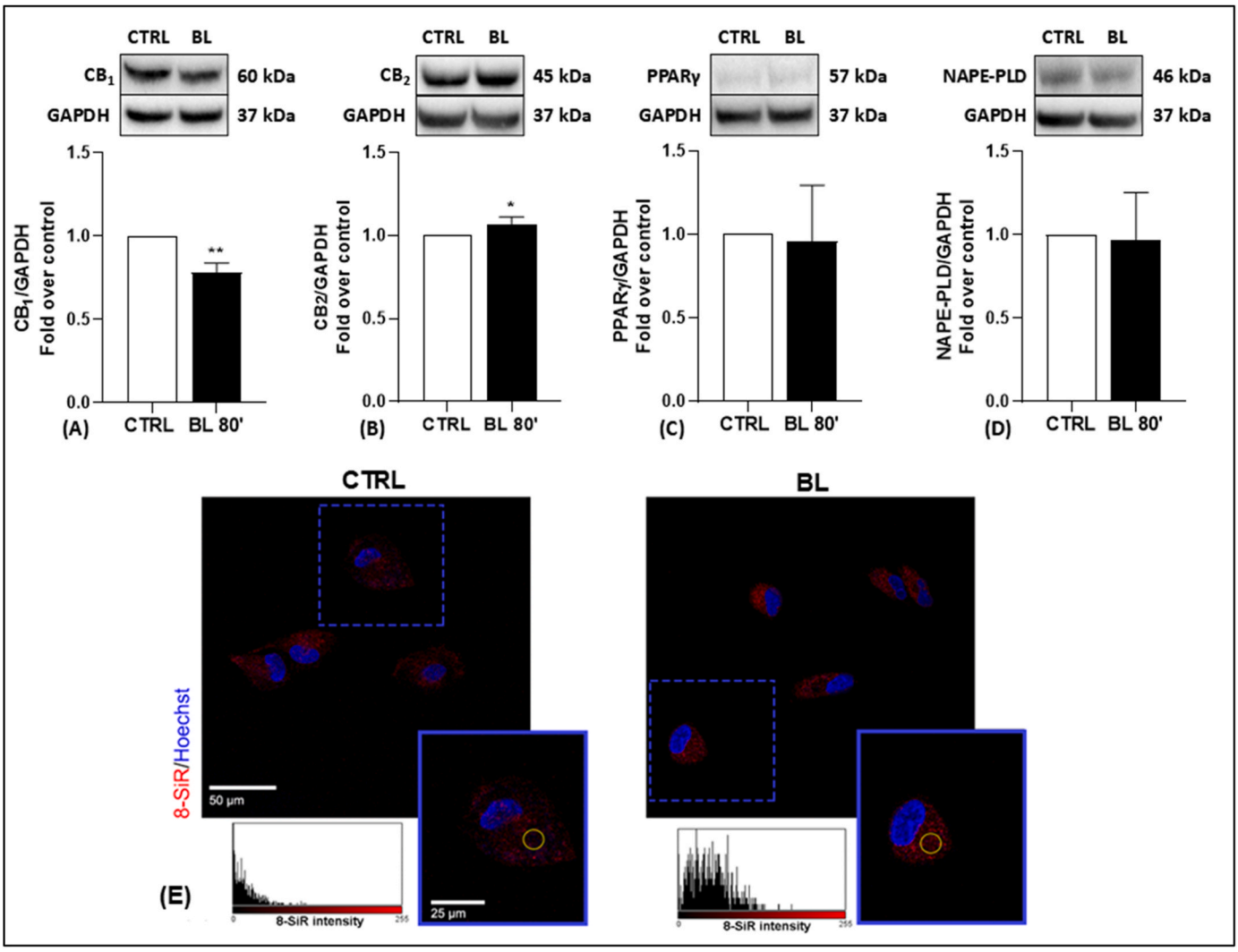

Fig. 4. BL effect on protein expression of selected ECS elements in ARPE-19 cells. Protein expression of **(A)** CB_1, **(B)** CB_2, **(C)** PPARγ **(D)** NAPE-PLD in BL and CTRL cells. Data are shown as the mean ± SEM of three independent experiments (N = 3). Statistical analysis was performed by Unpaired *t*-test (*p < 0.05 and **p < 0.01 *vs* CTRL). Representative bands of ECS components are shown above the reference histogram. **(E)** Representative confocal microscopy images of BL-treated and control ARPE-19 cells stained with the fluorescent 8-SiR probe for the visualization of intracellular CB_2 receptor (red) after 30′ of incubation with the probe; cells were counterstained with Hoechst nuclear dye (blue). The blue boxes show higher magnifications of ARPE-19 cells. The 8-SiR fluorescent profiles are representative of the yellow-highlighted area. Scale bars: 50 μm and 25 μm. Videos of the cell live imaging are available as Supplementary Material. (For interpretation of the references to color in this figure legend, the reader is referred to the Web version of this article.)

gene and protein expression of the major ECS elements in AMD-like ARPE-19 cells, supporting the use of this cell line for molecular investigations into the ECS in the RPE. Moreover, we demonstrate an unprecedented ECS dysregulation upon BL-induced damage, which may have implications for better understanding the molecular underpinnings of AMD.

CRediT authorship contribution statement

Camilla Di Meo: Writing – original draft, Validation, Software, Methodology, Investigation, Formal analysis, Data curation. **Annamaria Tisi:** Writing – original draft, Validation, Software, Methodology, Investigation, Formal analysis, Data curation. **Anna Rita Lizzi:** Software, Methodology, Investigation, Formal analysis, Data curation. **Sakthimala Palaniappan:** Software, Methodology, Investigation, Formal analysis, Data curation. **Fanny Pulcini:** Software, Methodology, Investigation, Formal analysis, Data curation. **Benedetta Cinque:** Software, Methodology, Investigation, Formal analysis, Data curation. **Simona Delle Monache:** Software, Methodology, Investigation, Formal analysis, Data curation. **Marc Nazarè:** Methodology. **Eric Hsu:** Resources. **Cinzia Rapino:** Writing – review & editing, Supervision, Project administration, Conceptualization. **Mauro Maccarrone:** Writing – review & editing, Supervision, Project administration, Funding acquisition, Conceptualization.

Fundings

This study was supported by InMed Pharmaceuticals Inc. (Vancouver, Canada) under a collaborative research agreement (CRA-AMD) with M.M. The funder had no role in the design of the study, in the collection, analyses or interpretation of data, nor in the decision to publish the results. The study was also partially funded by a competitive intramural grant of University of L'Aquila (Progetti di Ateneo 2021) to M.M.

Declaration of competing interest

All authors declare that they have no financial, personal, or professional relationships with other entities that could potentially influence

the work presented in this manuscript.

Acknowledgements

Part of the Graphical Abstract figure was drawn using pictures from Servier Medical Art, that is licensed under a Creative Commons Attribution 3.0 Unported License (https://creative commons.org/licenses/by/3.0/).

Appendix A. Supplementary data

Supplementary data to this article can be found online at https://doi.org/10.1016/j.bbrc.2025.151896.

References

[1] S. Zhang, J. Ren, R. Chai, S. Yuan, Y. Hao, Global burden of low vision and blindness due to age-related macular degeneration from 1990 to 2021 and projections for 2050, BMC Public Health 24 (2024), https://doi.org/10.1186/s12889-024-21047-x.
[2] Light-emitting diodes (LEDS): implications for safety, Health Phys. 118 (2020) 549–561, https://doi.org/10.1097/HP.0000000000001259.
[3] X. Ouyang, J. Yang, Z. Hong, Y. Wu, Y. Xie, G. Wang, Mechanisms of blue light-induced eye hazard and protective measures: a review, Biomed. Pharmacother. 130 (2020) 110577, https://doi.org/10.1016/j.biopha.2020.110577.
[4] A. Tisi, G. Carozza, A. Leuti, R. Maccarone, M. Maccarrone, Dysregulation of resolvin E1 metabolism and signaling in a light-damage model of age-related macular degeneration, Int. J. Mol. Sci. 24 (2023) 6749, https://doi.org/10.3390/ijms24076749.
[5] A. Tisi, L. Scipioni, G. Carozza, L. Di Re, G. Cimino, C. Di Meo, S. Palaniappan, F. D. Valle, F. Fanti, G. Giacovazzo, D. Compagnone, R. Maccarone, S. Oddi, M. Maccarrone, Alterations of endocannabinoid signaling and microglia reactivity in the retinas of AD -like mice precede the onset of hippocampal β-amyloid plaques, J. Neurochem. (2024) 16256, https://doi.org/10.1111/jnc.16256 jnc.
[6] A. Leuti, D. Fazio, M. Fava, A. Piccoli, S. Oddi, M. Maccarrone, Bioactive lipids, inflammation and chronic diseases, Adv. Drug Deliv. Rev. 159 (2020) 133–169, https://doi.org/10.1016/j.addr.2020.06.028.
[7] C.N. Serhan, Systems approach to inflammation resolution: identification of novel anti-inflammatory and pro-resolving mediators, J. Thromb. Haemostasis 7 (2009) 44–48, https://doi.org/10.1111/j.1538-7836.2009.03396.x.
[8] V. Chiurchiù, A. Leuti, M. Maccarrone, Bioactive lipids and chronic inflammation: managing the fire within, Front. Immunol. 9 (2018) 38, https://doi.org/10.3389/fimmu.2018.00038.
[9] M. Maccarrone, Deciphering complex interactions in bioactive lipid signaling, Molecules 28 (2023) 2622, https://doi.org/10.3390/molecules28062622.
[10] S. Oddi, L. Scipioni, A. Totaro, G. Giacovazzo, F. Ciaramellano, D. Tortolani, A. Leuti, R. Businaro, F. Armeli, A. Bilkei-Gorzo, R. Coccurello, A. Zimmer, M. Maccarrone, Beyond symptom management: FAAH inhibition as a path to mitigate alzheimer's disease progression, in: Mouse Models of Amyloidosis, 2024, https://doi.org/10.1101/2024.07.23.604774.
[11] V. Chiurchiù, L. Scipioni, B. Arosio, D. Mari, S. Oddi, M. Maccarrone, Anti-inflammatory effects of fatty acid amide hydrolase inhibition in monocytes/macrophages from alzheimer's disease patients, Biomolecules 11 (2021) 502, https://doi.org/10.3390/biom11040502.
[12] C. Rapino, D. Tortolani, L. Scipioni, M. Maccarrone, Neuroprotection by (Endo) Cannabinoids in Glaucoma and Retinal Neurodegenerative Diseases, vol. 16, 2018, pp. 959–970, https://doi.org/10.2174/1570159x15666170724104305. CN.
[13] M. Maccarrone, I. Bab, T. Bíró, G.A. Cabral, S.K. Dey, V. Di Marzo, J.C. Konje, G. Kunos, R. Mechoulam, P. Pacher, K.A. Sharkey, A. Zimmer, Endocannabinoid signaling at the periphery: 50 years after THC, Trends Pharmacol. Sci. 36 (2015) 277–296, https://doi.org/10.1016/j.tips.2015.02.008.
[14] J.-F. Bouchard, C. Casanova, B. Cécyre, W.J. Redmond, Expression and function of the endocannabinoid system in the retina and the visual brain, Neural Plast. 2016 (2016) 1–14, https://doi.org/10.1155/2016/9247057.
[15] P. Kumar, A. Nagarajan, P.D. Uchil, Analysis of cell viability by the MTT assay, Cold Spring Harb. Protoc. 2018 (2018), https://doi.org/10.1101/pdb.prot095505 pdb.prot095505.
[16] G. Carozza, A. Tisi, A. Capozzo, B. Cinque, A. Giovannelli, M. Feligioni, V. Flati, R. Maccarone, New insights into dose-dependent effects of curcumin on ARPE-19 cells, Indian J. Manag. Sci. 23 (2022) 14771, https://doi.org/10.3390/ijms232314771.
[17] J. Van Loenhout, L. Freire Boullosa, D. Quatannens, J. De Waele, C. Merlin, H. Lambrechts, H.W. Lau, C. Hermans, A. Lin, F. Lardon, M. Peeters, A. Bogaerts, E. Smits, C. Deben, Auranofin and cold atmospheric plasma synergize to trigger distinct cell death mechanisms and immunogenic responses in glioblastoma, Cells 10 (2021) 2936, https://doi.org/10.3390/cells10112936.
[18] N. Zhu, H. Wang, B. Wang, J. Wei, W. Shan, J. Feng, H. Huang, A member of the nuclear receptor superfamily, designated as NR2F2, supports the self-renewal capacity and pluripotency of human bone marrow-derived mesenchymal stem cells, Stem Cell. Int. 2016 (2016) 5687589, https://doi.org/10.1155/2016/5687589.
[19] C. Di Meo, D. Tortolani, S. Standoli, F. Ciaramellano, B.C. Angelucci, A. Tisi, S. Kadhim, E. Hsu, C. Rapino, M. Maccarrone, Cannabinol modulates the endocannabinoid system and shows TRPV1 -mediated anti-inflammatory properties in human keratinocytes, Biofactors 2122 (2024), https://doi.org/10.1002/biof.2122 biof.
[20] T. Gazzi, B. Brennecke, K. Atz, C. Korn, D. Sykes, G. Forn-Cuni, P. Pfaff, R.C. Sarott, M.V. Westphal, Y. Mostinski, L. Mach, M. Wasinska-Kalwa, M. Weise, B.L. Hoare, T. Miljuš, M. Mexi, N. Roth, E.J. Koers, W. Guba, A. Alker, A.C. Rufer, E.A. Kusznir, S. Huber, C. Raposo, E.A. Zirwes, A. Osterwald, A. Pavlovic, S. Moes, J. Beck, M. Nettekoven, I. Benito-Cuesta, T. Grande, F. Drawnel, G. Widmer, D. Holzer, T. van der Wel, H. Mandhair, M. Honer, J. Fingerle, J. Scheffel, J. Broichhagen, K. Gawrisch, J. Romero, C.J. Hillard, Z.V. Varga, M. van der Stelt, P. Pacher, J. Gertsch, C. Ullmer, P.J. McCormick, S. Oddi, H.P. Spaink, M. Maccarrone, D. B. Veprintsev, E.M. Carreira, U. Grether, M. Nazaré, Detection of cannabinoid receptor type 2 in native cells and zebrafish with a highly potent, cell-permeable fluorescent probe, Chem. Sci. 13 (2022) 5539–5545, https://doi.org/10.1039/d1sc06659e.
[21] A. Tisi, M. Feligioni, M. Passacantando, M. Ciancaglini, R. Maccarone, The impact of oxidative stress on blood-retinal barrier physiology in age-related macular degeneration, Cells 10 (2021) 64, https://doi.org/10.3390/cells10010064.
[22] J. Blasiak, Senescence in the pathogenesis of age-related macular degeneration, Cell. Mol. Life Sci. 77 (2020) 789–805, https://doi.org/10.1007/s00018-019-03420-x.
[23] R. Agrawal, P.K. Balne, X. Wei, V.A. Bijin, B. Lee, A. Ghosh, R. Narayanan, M. Agrawal, J. Connolly, Cytokine profiling in patients with exudative age-related macular degeneration and polypoidal choroidal vasculopathy, Investig. Ophthalmol. Vis. Sci. 60 (2019) 376, https://doi.org/10.1167/iovs.18-24387.
[24] T. Baba, D. Miyazaki, K. Inata, R. Uotani, H. Miyake, S. Sasaki, Y. Shimizu, Y. Inoue, K. Nakamura, Role of IL-4 in bone marrow driven dysregulated angiogenesis and age-related macular degeneration, Elife 9 (2020) e54257, https://doi.org/10.7554/eLife.54257.
[25] L. Schloesser, S.M. Klose, M.M. Mauschitz, Z. Abdullah, R.P. Finger, The role of immune modulators in age-related macular degeneration, Surv. Ophthalmol. 69 (2024) 851–869, https://doi.org/10.1016/j.survophthal.2024.07.009.
[26] T. Schwitzer, R. Schwan, K. Angioi-Duprez, A. Giersch, V. Laprevote, The endocannabinoid system in the retina: from physiology to practical and therapeutic applications, Neural Plast. 2016 (2016) 1–10, https://doi.org/10.1155/2016/2916732.
[27] S. Marquart, P. Zerr, A. Akhmetshina, K. Palumbo, N. Reich, M. Tomcik, A. Horn, C. Dees, M. Engel, J. Zwerina, O. Distler, G. Schett, J.H.W. Distler, Inactivation of the cannabinoid receptor CB1 prevents leukocyte infiltration and experimental fibrosis, Arthritis Rheum. 62 (2010) 3467–3476, https://doi.org/10.1002/art.27642.
[28] Y. Wei, X. Wang, L. Wang, Presence and regulation of cannabinoid receptors in human retinal pigment epithelial cells, Mol. Vis. 15 (2009) 1243–1251.
[29] M.A. Dwyer, D. Kazmin, P. Hu, D.P. McDonnell, G. Malek, Research resource: nuclear receptor atlas of human retinal pigment epithelial cells: potential relevance to age-related macular degeneration, Mol. Endocrinol. 25 (2011) 360–372, https://doi.org/10.1210/me.2010-0392.
[30] A. Erickson, S. Zhou, J. Luo, L. Li, X. Huang, Z. Even, H. Huang, H.-M. Xu, J. Peng, L. Lu, X. Wang, Genetic architecture of protein expression and its regulation in the mouse brain, BMC Genom. 22 (2021) 875, https://doi.org/10.1186/s12864-021-08168-y.
[31] C. Di Meo, D. Tortolani, S. Standoli, C.B. Angelucci, F. Fanti, A. Leuti, M. Sergi, S. Kadhim, E. Hsu, C. Rapino, M. Maccarrone, Effects of rare phytocannabinoids on the endocannabinoid system of human keratinocytes, Indian J. Manag. Sci. 23 (2022) 5430, https://doi.org/10.3390/ijms23105430.
[32] C. Vogel, G.M. Silva, E.M. Marcotte, Protein expression regulation under oxidative stress, Mol. Cell. Proteomics 10 (2011) 009217, https://doi.org/10.1074/mcp.M111.009217. M111.
[33] H. Zhang, H. Shen, C.J. Jordan, Q. Liu, E.L. Gardner, A. Bonci, Z. Xi, CB2 receptor antibody signal specificity: correlations with the use of partial CB2-knockout mice and anti-rat CB2 receptor antibodies, Acta Pharmacol. Sin. 40 (2019) 398–409, https://doi.org/10.1038/s41401-018-0037-3.
[34] B. Cécyre, S. Thomas, M. Ptito, C. Casanova, J.-F. Bouchard, Evaluation of the specificity of antibodies raised against cannabinoid receptor type 2 in the mouse retina, Naunyn-Schmiedebergs Arch Pharmacol 387 (2014) 175–184, https://doi.org/10.1007/s00210-013-0930-8.
[35] R. Maccarone, C. Rapino, D. Zerti, M. di Tommaso, N. Battista, S.D. Marco, S. Bisti, M. Maccarrone, Modulation of Type-1 and Type-2 cannabinoid receptors by saffron in a rat model of retinal neurodegeneration. https://doi.org/10.1371/journal.pone.0166827, 2016.